Drug Development and Industrial Pharmacy, 33:79–90, 2007

ISSN: 0363-9045 print / 1520-5762 online
DOI: 10.1080/03639040600975030

informa
healthcare

Evaluation and Controlled Release Characteristics of Modified Xanthan Films for Transdermal Delivery of Atenolol†

Raghavendra C. Mundargi and Sangamesh A. Patil
Department of Chemistry
Center of Excellence in Polymer Science, Karnatak University, Dharwad, India

Sunil A. Agnihotri and Tejraj M. Aminabhavi
Drug Delivery Division, Center of Excellence in Polymer Science, Karnatak University, Dharwad, India

ABSTRACT The present study was performed to evaluate the possibility of using modified xanthan films as a matrix system for transdermal delivery of atenolol (ATL), which is an antihypertensive drug. Acrylamide was grafted onto xanthan gum (XG) by free radical polymerization using ceric ion as an initiator. Fourier transform infrared spectroscopy and differential scanning calorimetry indicated the formation of the graft copolymer. The obtained graft copolymer was loaded with ATL and films were fabricated by solution casting method for transdermal application. Various formulations were prepared by varying the grafting ratio, drug loading, and different penetration enhancers. The formulations prepared were characterized for weight, thickness uniformity, water vapor transmission rate, and uniformity in drug content of the matrix. All the thin films were slightly opaque, smooth, flexible, and permeable to water vapor, indicating their permeability characteristics suitable for transdermal studies. Fourier transform infrared spectroscopy and differential scanning calorimetry studies indicated no significant interactions between drug and polymer. Drug is distributed uniformly in the matrix but showed a slight amorphous nature. Drug-loaded films were analyzed by X-ray diffraction to understand the drug polymorphism inside the films. Scanning electron microscopic studies of the placebo and drug-loaded films demonstrated a remarkable change in their surface morphology. The skin irritation tests were performed in mice and these results suggested that both placebo and drug-loaded films produced negligible erythema and edema compared to formalin (0.8% v/v) as the standard irritant. The in vitro drug release studies were performed in phosphate buffer saline using a Keshary-Chien diffusion cell. Different formulations were prepared and variations in drug release profiles were observed. Release data were analyzed by using the Ritger and Peppas equation to understand the mechanism of drug release as well as the estimation of n values, which ranged between 0.41 and 0.53, suggesting a Fickian diffusion trend.

KEYWORDS Transdermal delivery system, Atenolol, In vitro release, Polysaccharide, Polyethylene glycol-6000

†This paper is Center of Excellence in Polymer Science Communication # 127.
Address correspondence to Tejraj M. Aminabhavi, Drug Delivery Division, Center of Excellence in Polymer Science, Karnatak University, Dharwad 580 003, India; Fax: 91-836-2771275; E-mail: aminabhavi@yahoo.com

INTRODUCTION

Transdermal drug delivery (TDD) offers several advantages over the most common routes of drug administration. One of the major advantages of the transdermal therapeutic system (TTS) is the maintenance of blood concentration of a drug at the desired therapeutic level by the controlled permeation of drug through the skin. The discipline of TDD has experienced a tremendous growth over the past decade, because of the increasing number of drugs that can be delivered to the systemic circulation in clinically effective concentrations via the skin portal. This is possible despite the inherent protective function of the stratum corneum, which is primarily one of the excluding foreign substances from entering the body. Success has been achieved in administering several drugs transdermally using TTSs with a view to maintain a constant plasma concentration of the respective drug over the predetermined time period (Shin & Choi, 2003).

Formulation of TTSs involves the optimization of several factors such as release rate, stability, safety, convenience of use, etc. However, the key component in a TTS, which monitors the release of an active ingredient, is the rate controlling judicially chosen polymeric membrane. The polymer should possess good film forming properties, should be nonirritating, inert, and stable. Hence, the selection of a polymer is quite difficult because of the inherent diversity of structures, which requires thorough understanding of the surface and bulk properties of the polymer that can offer desired chemical, interfacial, mechanical, and biological functions. Even though several polymers are already in use, yet new polymers to develop TTS are still the need of the day. However, one of the major disadvantages of TDD as compared to other controlled release (CR) formulations is its high cost.

Transdermal patches are of two types: membrane controlling and matrix type systems (Valenta & Auner, 2004). Membrane systems are constructed of rate controlling membranes, whereas in matrix controlled systems, the drug is dissolved or suspended in a hydrophilic or lipophilic matrix. Flexibility and plasticization of the films to be developed can be achieved by modification/blending with another polymer, cross-linking, etc. In addition to being biocompatible, the advantages of such systems are that an additional free volume space can be created to accommodate the drug without any hindrance during its slow release from the matrix. Polyacrylamide-based hydrogel type transdermal device has been reported (Banga & Chien, 1993) for the transdermal delivery of peptides and calcitonin, but it was found necessary to improve the permeation rate of drugs by using suitable penetration enhancers that can rapidly and reversibly promote the percutaneous penetration of drugs. However, the most frequently used penetration enhancers are alcohols, fatty acids, surfactants, azones, and terpenes. Surfactant facilitated permeation of drugs through skin membranes has been studied (Sarpotdar & Zatz, 1986; Williams & Barry, 2004) giving reports of significant enhancement of drugs like chloramphenicol through hairless mouse skin by sodium lauryl sulfate and acceleration of hydrocortisone and lidocaine permeating across the hairless mouse skin by the nonionic surfactant, Tween® 80.

Atenolol (ATL) is a beta-adrenergic receptor blocking agent without membrane stabilizing or intrinsic sympathomimetic activities. It has been used for the treatment of hypertension and stable angina either alone or with other antihypertensive drugs like thiazide diuretics. It is reported that in oral applications, it can induce side effects like diarrhea, nausea, ischemic colitis, and mesenteric arterial thrombosis. ATL is reported to be subjected to extensive hepatic first-pass metabolism following the oral administration and has a short biological half-life. The development of TDD containing antihypertensive drug and maintaining proper blood level for a long time without any adverse effects of frequent oral administration is very important (Kim & Shin, 2004; Cho & Shin, 2004). Therefore, it is desirable to develop a TDD system containing ATL as a model drug. As a further contribution in this area, we report here the development of transdermal films using modified xanthan gum (XG) obtained by grafting acrylamide onto XG (i.e., AAm-*g*-XG) with ceric ion as an initiator and fabrication of transdermal films for the CR of ATL. The grafted copolymer and fabricated placebo as well as drug-loaded films have been characterized by thermal analysis. The in vitro release studies were performed in phosphate buffer saline (PBS, pH 7.4) at 37°C using a Keshary-Chien diffusion cell for up to 24 hr. These results have been fitted to empirical equation proposed by (Ritger & Peppas, 1987) to understand the release mechanism. Such release data are important in further development of similar systems by selecting a proper drug-polymeric matrix.

MATERIALS

ATL and XG were obtained as gift samples from Medreich Sterilab Ltd. and Himalaya Drug Co., Bangalore, India. Acrylamide (AAm), acetone, ceric ammonium nitrate (CAN), polyethylene glycol (PEG-6000), and Tween®80 were all purchased from s.d. Fine Chemicals, Mumbai, India. Dialysis Membrane-110 was purchased from Himedia Laboratories Pvt. Ltd., Mumbai, India. Pluronic F127 was purchased from Aldrich Chemical Company, Inc. (Milwaukee, WI). Throughout the study, double distilled water was used.

METHODS

Synthesis of Graft Copolymer

The graft copolymer derived from AAm and XG was prepared by free radical polymerization. Briefly, 1.0 g of XG was dispersed in 120 mL of water and dissolved overnight under constant stirring in a 250 mL round bottom flask. Then, three different amounts, viz., 7.5, 10.0, or 12.0 g of AAm were mixed with 30 mL of water, added to XG solution and stirred for 1 hr. A quantity of initiator equivalent to 0.05 mmol was dissolved in 30 mL of water and added to the above solution. Polymerization was performed at 60°C under the continuous purging of nitrogen gas for 4 hr in a thermostatic water bath with constant stirring. After complete polymerization, the reaction mixture was cooled by running under tap water and poured into excess acetone to induce precipitation. The graft solid polymer formed was washed several times with methanol: water (80:20, v/v) mixture, distilled water to remove the unreacted monomer and reagents and then vacuum dried at 40°C to a constant weight. The percentage grafting (% G), grafting efficiency (% GE), and percentage conversion (% C) were calculated by using:

$$\%\ Grafting\ (\%\ G) = \left(\frac{W_1 - W_0}{W_0}\right)100 \quad (1)$$

$$\%\ Grafting\ efficiency\ (\%\ GE) = \left(\frac{W_1 - W_0}{W_2}\right)100 \quad (2)$$

$$\%\ Conversion\ (\%\ C) = \left(\frac{W_1}{W_2}\right)100 \quad (3)$$

where W_0, W_1, and W_2 denote the weights of XG, graft copolymer, and AAm, respectively.

Preparation of ATL-loaded Transdermal Films

The films developed were from the modified XG containing PEG-6000 as a plasticizer and formulated to contain graft copolymer of various grafting ratios (1:7.5, 1:10, and 1:12) and different drug loadings (20%, 30%, and 40%) with two different penetration enhancers. In order to understand the variables, formulation codes were assigned as given in Table 1. For instance, the formulation code, F1P1, F1P2, and F1P3 refers to grafting ratios. Formulations F1P1, F2P2, and F2P3 represent the drug loading, F3P1, F3P2 refer to the penetration enhancers. The films were prepared by solution casting and solvent evaporation method. The graft copolymer, plasticizer (20% w/w of dry weight of graft copolymer), penetration enhancer (20% w/w of dry weight of graft copolymer) and drug were all dissolved in distilled water and stirred thoroughly to get

TABLE 1 **Transdermal Films: Polymers and Their Compositions**

Formulation code	Graft copolymer (mg)	Drug (%)	Plastisizer (mg)	Penetration enhancer
F1P1	300 (1:7.5)	20	100	–
F1P2	300 (1:10)	20	100	–
F1P3	300 (1:12)	20	100	–
F2P2	300 (1:7.5)	30	100	–
F2P3	300 (1:7.5)	40	100	–
F3P1	300 (1:7.5)	20	100	Pluronic F127
F3P2	300 (1:7.5)	20	100	Tween®80

a homogeneous solution. This bubble-free solution was casted on petri dish plates lined with aluminum foil. The films were air-dried in dust-free environment for 48 hr and stored in a desiccator until further evaluation. There was no change in the physical appearance or texture of the films even after storage. The drug-loaded polymeric films were characterized for film thickness, weight variation, folding endurance, water permeation, and drug content. Thickness of the films was measured by a micrometer at five different places on the film and average thicknesses were recorded.

Folding Endurance

This was determined by repeatedly folding the film at the same place until it broke. The number of times the film could be folded at the same place without breaking/cracking gave the value of folding endurance.

Estimation of ATL in the Films

Films with a specified area (1.32 cm^2) were cut into small pieces and put into a 100–mL volumetric flask. About 50 mL of PBS with pH 7.4 was added and kept for 24 hr with occasional shaking. Then, the volume was made up to 100 mL with PBS. Similarly, a blank was performed by using a drug-free patch. The solutions were filtered and absorbance was measured at the λ_{max} value of 226 nm using a UV spectrophotometer (Secomam, Anthelie, France).

Permeability Measurement

Water vapor transmission (WVT) studies were performed according to the method proposed by Rao and Diwan (Rao & Diwan, 1997) using glass vials of equal diameter as the transmission cells. These cells were washed and dried in an oven. About 1 g of fused calcium chloride was taken in the cells and polymeric patches (1.7 cm^2 area) were fixed over the brim with the help of an adhesive. Then, cells were accurately weighed and kept in a closed desiccator containing the saturated solution of potassium chloride (200 mL). Humidity inside the desiccator was measured by a hygrometer; the relative humidity (RH) was found to be 84%. The cells were removed and weighed every day for 7 days of the storage period. The WVT data through transdermal films are important in knowing the permeation characteristics of the films. The WVT rates were calculated using the formula:

$$\text{Transmission rate} = WL / S \quad (4)$$

where W is weight of water transmitted in g/cm^2/24 hr, L is thickness of the film, and S is exposed surface area of the film. WVT of the films varied from 1.6×10^{-3} to 8.0×10^{-4} g/cm^2/24 hr. These results indicated that films were permeable to water vapor. The WVT of cellulose acetate films prepared from 2% w/v casting solution was reported (Rao & Diwan, 1997) to be 11.9×10^{-3} g/cm^2/24 hr. These films were found to be suitable for developing formulation of TDD systems. Properties of the modified xanthan films were comparable with cellulose acetate films.

Fourier Transform Infrared (FT-IR) Spectral Studies

AAm, XG, AAm-*g*-XG, ATL, and the drug-loaded films were analyzed by FT-IR to confirm the grafting reaction and chemical interactions between the drug and the polymeric matrix using the KBR pellet technique. Spectra were scanned on a Nicolet, Model Impact 410, Milwaukee, in the range of 500–4000 cm^{-1}.

Differential Scanning Calorimetric Analysis

Differential scanning calorimetric (DSC) experiments were performed on XG, AAm-*g*-XG, pristine drug, placebo film, and drug-loaded film by using a Rheometric Scientific, DSC SP, Surrey, UK, thermal analyzer. Samples were heated at the rate of 10°C/min from ambient temperature to 400°C under an inert nitrogen atmosphere at the flow rate of 10 mL/min.

X-Ray Diffraction (X-RD) Studies

X-ray diffraction studies were performed on pristine drug, placebo film, and drug containing film using the powder X-RD technique with Philips model PW-1710 diffractometer attached to a digital graphical assembly and computer with Cu-NF 25 KV/20-mA tube as the Cuα-radiation source in the range of 0°–50° of 2θ.

Scanning Electron Microscopic Studies

Scanning electron microscopy (SEM) was used to study the surface morphology of placebo and drug-loaded films. Samples were coated with gold-palladium for 60 s under an argon atmosphere. Scanning was done using JEOL model JSM-840A, Japan. These data were collected at UT Southwestern Medical Center at Dallas, TX.

In Vitro Drug Release Study

In vitro drug release was performed in PBS using a Keshary-Chien diffusion cell. The appropriate size of polymeric patches (area exposed to donor compartment was 1.32 cm^2) were mounted between the donor and the receptor compartments of the diffusion cell (using dialysis membrane as a permeation barrier) and were held securely by springs. The donor compartment was empty and open to air, while the receptor compartment was filled with PBS and stirred at 100 rpm rotation speed. The whole assembly was maintained at 37°C using a thermostatic water bath (Grant, UK). The amount of drug released was determined by withdrawing 1 mL aliquots at the selected specified time intervals up to 24 hr. The volume withdrawn was replaced with an equal volume of fresh and pre-warmed PBS at 37°C. Samples were analyzed by UV spectrophotometer (Secomam, Anthelie, France) at the λ_{max} value of 226 nm using PBS as the blank.

Skin Irritation Studies

The mice were divided into five groups (n=6). On the previous day of the experiment, the hair on the backside area of the mice was removed. The animals of group I were served as normal, without any treatment. One group of animals (Group II, control) was applied with a marketed adhesive scotch tape (official adhesive tape in USP). Transdermal systems (placebo and drug-loaded) were applied onto the nude skin of the animals of III and IV groups. A 0.8% v/v aqueous solution of formalin was applied as a standard irritant (Group V). Animals were applied with new patch/formalin solution each day up to 7 days and finally the application sites were graded according to a visual scoring scale: 0 for none, 1 for slight, 2 for well defined, 3 for moderate, and 4 for scar formation. The edema scale was: 0 for none, 1 for slight, 2 for well defined, 3 for moderate, and 4 for severe.

RESULTS AND DISCUSSION

Synthesis of Poly(acrylamide)-*grafted*-Xanthan Gum

In the present study, we have attempted to synthesize the graft copolymer by using ceric ion. The reaction conditions were standardized to minimize homopolymerization as well as to give better yield. The reactive vicinal group where the grafting is initiated on the XG backbone is CH_2OH. The overall reaction mechanism is that ceric ion attacks the XG macrochains and generates the formation of a XG–ceric complex. The ceric(IV) ions in the complex are then reduced to ceric(III) ions by oxidizing hydrogen atom and thereby, creating a free radical onto the XG backbone. The grafting of poly(acrylamide) (pAAM) onto XG is then initiated by the free radical reacting with the monomer. In the presence of pAAM, the XG free radical is chemically coupled to the monomer unit, thereby resulting in a covalent bond between pAAM and XG to create a chain reaction for propagation. Finally, termination is achieved through a combination of two radicals. The earlier methods (Behari et al., 2001; Adhikary & Singh, 2004) reported the synthesis of graft copolymerization of AAm onto XG initiated by the Fe^{2+}/BrO_3^- redox system and CAN as the catalyst in an aqueous medium. Details of the reaction scheme were given in our earlier report (Mundargi et al., 2006). Synthetic details are summarized in Table 2. The percentage grafting varied from 566 to 1051 and the monomer conversion was increased with increasing the ratio of AAm to XG. In the present study, the reaction mixture was precipitated in acetone and washed several times with methanol:water (80:20, v/v) mixture and finally, with distilled water to remove the unreacted monomer and the unwanted reagents. Hence, the presence of ceric ions and homopolymers are excluded. As far as toxicology is concerned, as per the investigation made by Jakupec et al. (2004), it was observed that Ce(IV) salts are not biologically stable in the aqueous media. Therefore, cerium species that circulate in the blood as colloidal compounds or protein complexes are likely to contain Ce(III). The close similarity of the ionic radii of Ce^{3+} (1.01 Å) and Ca^{2+} (1.00 Å) allows Ce^{3+}

TABLE 2 Synthetic Details of Polyacrylamide-*grafted*-Xanthan Gum

Code	Mass of XG (g)	Mass of AAm (g)	Mass of initiator (mmole)	% Yield	% Grafting	% Grafting efficiency	% Conversion
XG1	1	7.5	0.05	78.35	566	75.46	88
XG2	1	10	0.05	84.45	829	82.90	92
XG3	1	12	0.05	88.53	1051	87.58	96

(and other light Ln^{3+} ions) to replace Ca^{2+} ions in the biomolecules.

Several drug-loaded pAAM hydrogels have also been used for in vitro studies. In addition, in vivo systems have been explored for the AAm-based matrices in developing superporous hydrogels. Notice that AAm blended hydrogels were found to be biocompatible (Karadag et al., 1996). In a study by Makarand & Bhonde (2000), the in vitro cytotoxicity by MTT, a mitochondrial assay and NR, a lysosomal functionality assay showed no toxic effects on NIH3T3 and HeLa cells up to 40% of hydrogel extract, thus supporting the earlier observations about the biocompatibility of starting polymers. Thus, high viability of NIH3T3 and HeLa cells upon exposure to hydrogel will leach out the extracts as an indication of good tolerance of the hydrogel.

Preparation of Drug-loaded Transdermal Films

Monolithic matrix type TTS loaded with ATL were prepared by solution casting method. In all, seven formulations were prepared by varying three parameters, viz., grafting ratio, drug loading, and penetration enhancers as shown in Table 1. PEG-6000 is used in concentrations of 20% w/w as a plasticizer; polymeric films with concentrations less than 20% w/w plasticizer were somewhat brittle and lacked the folding endurance. However, the films with a plasticizer concentration above 30% w/w did not further improve the film properties (compared to those prepared with 20% w/w). Hence, 20% w/w was fixed as the optimum concentration for the plasticizer. The surfactant Tween® 80 and Pluronic F127 were used as the penetration enhancers. Various trials were taken to optimize the formulation to get the desired thickness, flexibility, drug loading, and release profile.

Physicochemical Characterization of the Films

Physicochemical properties of the films are summarized in Table 3. The films formed were slightly opaque and had uniform thicknesses varying from 0.082 to 0.112 mm. Drug content of the films varied from 94.26 to 98.17%. The process employed to prepare films in this study was capable of producing films with a uniform drug content and a minimum batch variability. Weight of the completely dried film was recorded in the range of 1.13 to 2.39 mg. Folding endurance was varied from 21 to 32; formulations F1P3 and F3P2 exhibited maximum and minimum folding endurances, respectively.

Fourier Transform Infrared Spectroscopy

Grafting of AAm onto XG was confirmed by FT-IR studies. FT-IR spectra of (a) AAm, (b) AAm-*g*-XG, and

TABLE 3 Physicochemical Properties of the Transdermal Films

Formulation code	Thickness (mm)	Weight (mg)	WVT (g/cm^2/24 hr)	Folding endurance	Drug content (%)
F1P1	0.102	1.80	1.60×10^{-3}	22	97.26
F1P2	0.112	2.00	1.35×10^{-3}	24	98.24
F1P3	0.111	2.39	1.60×10^{-3}	32	96.98
F2P2	0.102	1.70	1.50×10^{-3}	28	96.54
F2P3	0.100	2.04	8.00×10^{-4}	29	94.26
F3P1	0.096	1.45	1.08×10^{-3}	23	98.17
F3P2	0.082	1.13	1.25×10^{-3}	21	95.16

(c) XG are displayed in Fig. 1. In case of pure XG, a broad absorption peak at 3450 cm^{-1} indicates the presence of hydrogen-bonded OH groups. Two peaks, one at 1615 cm^{-1} and the other at 1476 cm^{-1}, are attributed to COO^- groups. Additional characteristic absorption bands of XG appear at 1417 and 1023 cm^{-1} because of the C-H and O–H bending vibrations, respectively. In the FT-IR spectrum of AAm, a characteristic absorption band observed at 3355 cm^{-1} is attributed to N–H stretching, whereas the bands appearing at 1673 and 1610 cm^{-1} are caused by the amide stretching vibrations. Additional characteristic absorption bands of AAm appear at 1425 and 1350 cm^{-1}, respectively, because of the O–H bending and C–O stretching vibrations. In the case of graft copolymer of AAm-*g*-XG, the bands at 1675 and 1635 cm^{-1} are, respectively, attributed to amide-I (C–O stretching) and amide-II (N–H bending) of the amide group of AAm. The peak at 3421 cm^{-1} in AAm-*g*-XG matrix is attributed to a overlap of N–H stretching band of the amide group and O–H stretching band. The C–N stretching band appears at 1450 cm^{-1}. These factors are the effective evidence for the successful grafting reaction.

FT-IR spectra of the pristine ATL (curve a) and the drug-loaded film (curve b) are presented in Fig. 2. ATL showed characteristic bands because of the different functional groups. However, the band appearing at 3356 cm^{-1} is attributed to O–H/N–H stretching vibrations, while those observed at 2924 and 2963 cm^{-1} are caused by the aliphatic C–H stretching vibrations. The band at 3175 cm^{-1} is because of aromatic C–H stretching vibrations, whereas those appearing at 1637 and 1583 cm^{-1} are caused by the primary amide bond stretching and aromatic C=C stretching vibrations, respectively. The N–H bending vibrations are seen at 1516 cm^{-1}. Bands at 1180 and 1092 cm^{-1} are attributed to the C–O–C stretching vibrations of the ether linkages. The C–N stretching vibrations are seen at 1037 cm^{-1}, while the one that appeared at 1243 cm^{-1} is attributed to aromatic C–O stretching vibrations. The peaks appearing at 3349, 2971, 2924, 1639, 1519, 1249, and 1041 cm^{-1} for ATL have also appeared in the ATL-loaded films, indicating the chemical stability of ATL in the chosen polymeric matrix. This also indicates that ATL is not involved in any chemical reactions with either the polymer or the excipients used.

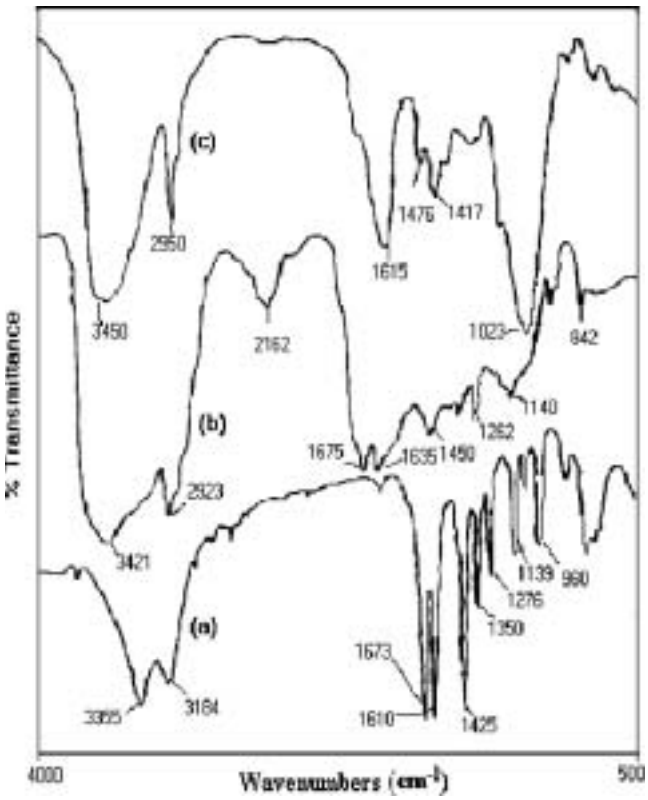

FIGURE 1 FT-IR Spectra of (a) AAm, (b) AAm-*g*-XG, and XG.

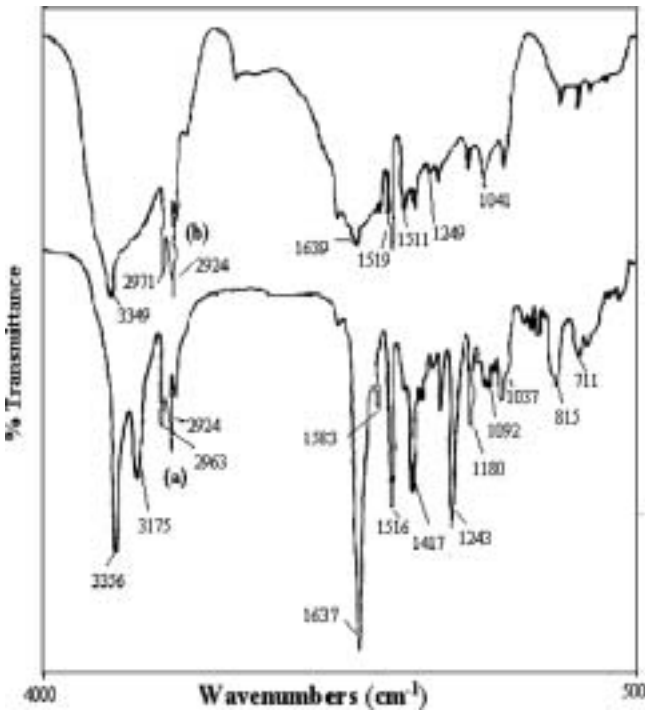

FIGURE 2 FT-IR Spectra of (a) Pristine Drug and (b) Drug-loaded Film.

Differential Scanning Calorimetry

DSC is a useful technique to explain the formation of graft copolymers. DSC curves of XG (a) and graft copolymer (b) are reproduced in Fig. 3. XG showed an endothermic transition at 65°C, whereas the graft copolymer exhibited two endothermic transitions, one at 70°C and another at ~360°C. The new endothermic transition observed at 360°C in the thermogram of the graft copolymer may be caused by the enhanced interaction between carbonyl groups of the grafted copolymer and hydroxyl groups of XG. These results confirm the grafting of AAm onto XG.

DSC scans of the pristine drug, placebo film, and the drug-loaded film are presented in Fig. 4. The endothermic peaks of ATL appeared at its melting point, 158°C (curve a), which appears at 152°C in the DSC plots of the ATL-loaded film (curve c) with a much lesser intensity. A slight shifting of the peak indicates no recrystallization of the pristine drug within the polymer matrix as a result of the molecular interactions between the drug and the polymer. This further confirms a uniform dispersion of ATL in the polymer matrix. The placebo film (curve b) has shown two endothermic transitions at 267 and 358°C, but no peak was observed near the endothermic peak exhibited by the pristine drug. Endothermic peaks of the placebo film, after loading the drug, decreased to 184°C because of the possible formation of the loose polymer network as a result of the creation of extra free space after drug loading. These results suggest the absence of any interactions between the polymer matrix and the ATL.

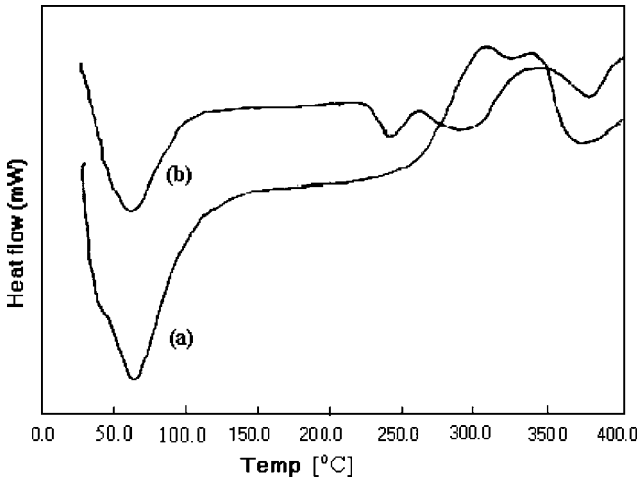

FIGURE 3 DSC Thermograms of (a) XG and (b) AAm-*g*-XG.

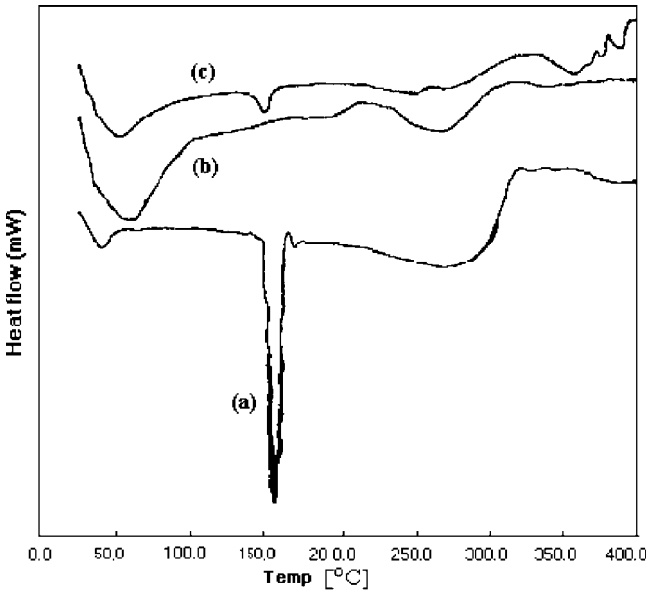

FIGURE 4 DSC Thermograms of (a) Pristine Drug, (b) Placebo Film and (c) Drug-loaded Film.

X-Ray Diffraction

The X-ray diffraction patterns of pristine drug (curve a), drug-loaded film (curve b), and placebo film (curve c) are presented in Fig. 5. The placebo film

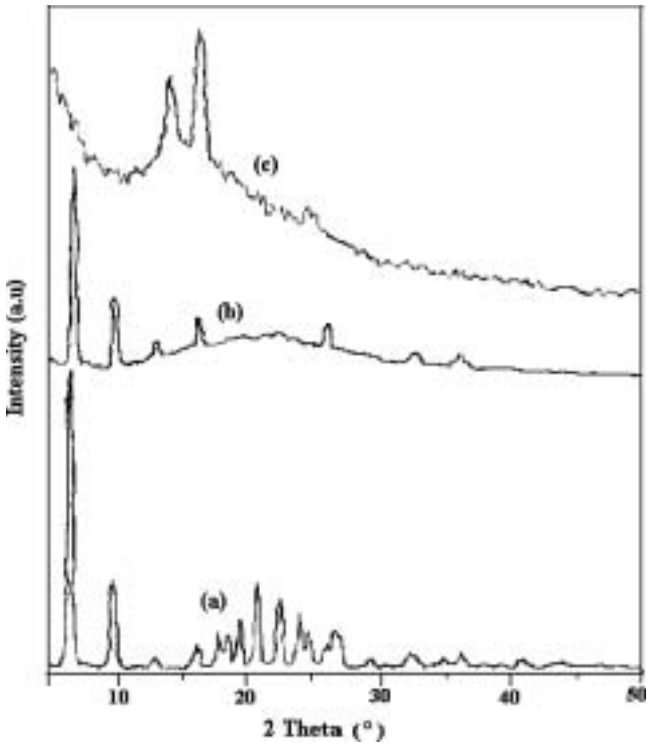

FIGURE 5 X-RD Diffractograms of (a) Pristine Drug, (b) Drug-loaded Film and (c) Placebo Film.

shows two peaks, one at 14.18° and the other at 16.32°. Diffractogram of the ATL shows many characteristic sharp peaks. The highest crystalline ATL peaks occurred at 2θ of 6.33°, 6.53°, 9.56°, 20.64°, and 20.75°, and series of smaller peaks are observed at 2θ angles of 16.04°, 19.29°, 22.32°, 24.68°, and 26.46°. In the case of drug-loaded film, only the peaks at 6.52°, 9.74°, 16.21°, and 26.09° were observed, but the peak intensities were smaller when compared to the pristine drug, indicating that the drug-loaded inside the polymer matrix is not completely in its crystalline form. This further confirms that a portion of the drug is molecularly dispersed in the polymer matrix film.

Scanning Electron Microscopy

Scanning electron microscopy was used to examine the surface morphology of the films. SEM images of the placebo films and the drug-loaded films are shown in Fig. 6. The placebo films exhibited a clear and homogenous surface, whereas drug-loaded films showed a uniform distribution of ATL in the polymeric matrix.

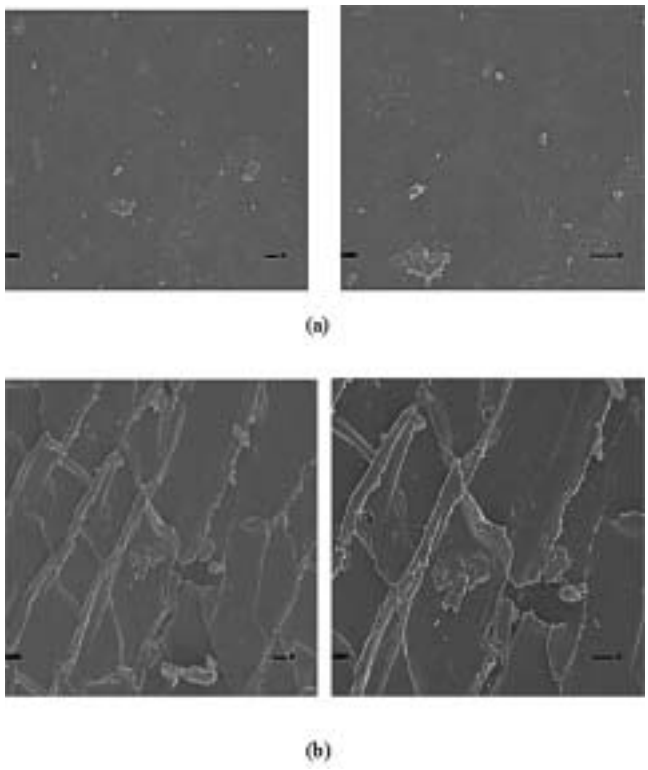

FIGURE 6 SEM Images of (a) Placebo Films and (b) Drug-loaded Films.

Skin Irritation Studies

Skin irritation studies were performed to investigate the potential for ATL and the polymeric matrix to cause irritant or allergic reactions, which are usually produced by a specific base component. Many test protocols are described to study the irritancy levels, both in animals and humans (Wilkinson & Moore, 1989). The results depicted in Table 4 indicate that the polymeric film (placebo and drug-loaded) as well as the USP adhesive tape produced negligible erythema and edema. On the other hand, the standard irritant, viz., formalin was found to produce severe erythema and edema effects.

In Vitro Release Studies

The in vitro drug release studies were performed in PBS at 37°C using Keshary-Chien diffusion cell with dialysis membrane acting as the diffusion barrier. The in vitro release profiles of formulations containing graft copolymer of grafting ratios are displayed in Fig. 7. Notice that formulation F1P1 releases the maximum amount of drug as compared to other formulations, i.e., it released about 90% of the drug in about 24 hr, whereas the formulations F1P2 and F1P3 released 88% and 84%, respectively under similar conditions. It is interesting to note that with increasing grafting ratio of the copolymer, a slight decrease in release rate of the drug occurred, suggesting that the release depends upon the chain length of pAAm part of the copolymer. Thus, by varying the grafting ratio, the amount of XG in the copolymer will change and the length of the side chain of the copolymer will increase. This will greatly affect the release patterns in all the grafted copolymers. The observed initial rapid release rate may be accounted for by the direct exposure of the membrane system to the diffusion media with a quick release of the drug present at the surface (Brazel & Huang, 2001) and such an initial rapid

TABLE 4 Results of Skin Irritation Tests

Formulation	Erythema	Edema
Normal	0.00	0.00
Adhesive tape (USP)	1.72	1.61
Drug loaded	1.48	1.31
Placebo	1.08	1.28
Formalin (0.8% v/v)	3.12	3.29

release is attributed to the fact that polymeric matrix may form loose channels within the network, because of its hydrophilic nature and the dissolution of hydrophilic polymers during the diffusion process. The formation of such loose channels leads to a decrease in the mean diffusional path length of the drug molecule to leach out into the diffusion medium, thereby resulting in the higher rates of drug release from the membrane matrix. The observed initial release may be helpful to achieve the therapeutic plasma concentration of the drug in a short time along with a constant release rate at longer time period, providing CR of the drug. However, such an initial effect is related to the initial migration of the drug particles toward the surface of the membrane matrix.

The effect of drug loading on release rate from xanthan films was studied at 37°C for 24 hr with different drug loadings of 20%, 30%, and 40% (w/w) into the matrix. The in vitro release profiles at various drug loadings are depicted in Fig. 7. The total amount of drug released from F2P3 formulation is about 95% at the end of 24 hr, whereas formulations F1P1 and F2P2 released 89% and 94%, respectively. ATL is a hydrophilic drug, which will, therefore, exert an interaction with the water-soluble polymers, resulting in an increase of drug release. Also, the hydrophilic XG will readily absorb water molecules and will swell, resulting in the formation of large pores. Thus, as the drug loading increased, the release rate also increased. Increased release rate and the extent of drug release are attributed to the increase in the rate of diffusion at higher concentrations of the drug. Similar observations were reported earlier by Kim & Shin (2004). In the present study, two different penetration enhancers were used. The release profiles of these formulations are shown in Fig. 7, which indicated a slight enhanced release for formulations F3P1 and F3P2, respectively containing Pluronic F127 and Tween® 80 than the control.

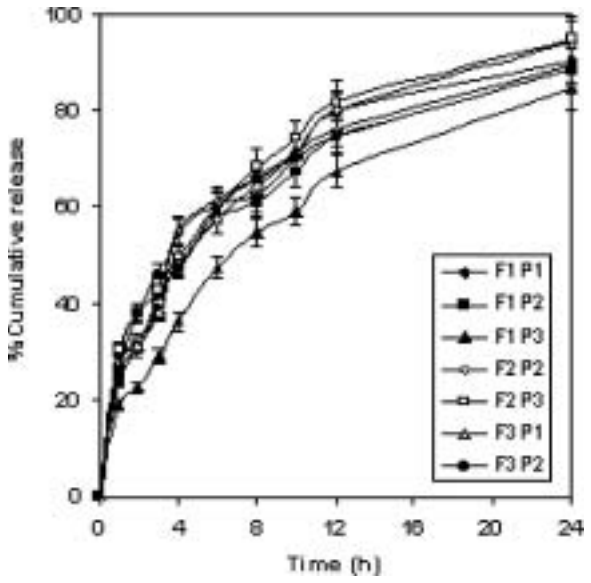

FIGURE 7 **Effect of Grafting Ratio, Drug Loading, and Penetration Enhancers on In Vitro Release Profile.**

The results of fractional release (M_t/M_∞) have been analyzed using an empirical equation (Ritger & Peppas, 1987):

$$\frac{M_t}{M_\infty} = Kt^n \tag{5}$$

Here the values of n represent the diffusion anomalies and K is an empirical parameter representing the interaction between drug and the polymer. Estimated values of n along with correlation coefficient, r values are presented in Table 5. In case of drug release from the swellable matrices, if n=0.5, it indicates that transport follows the Fickian trend. For all formulations studied in this work, the values of n ranged between 0.41 and 0.53, suggesting that diffusional transport follows a Fickian trend. In case of Fickian diffusion, the rate of water absorption increases linearly when plotted as a function of time. Fickian diffusion is observed when the time scale of the macromolecular relaxation is either effectively infinite or zero as compared to the time required to establish a concentration profile in the polymer (Peppas & Khare, 1993). These two signify the elastic and viscous Fickian diffusion limits. Matrix systems reach an equilibrium state of relaxation extremely fast with a Fickian diffusion of the drug being the dominant drug transport mechanism.

TABLE 5 **Results of Flux, Permeability Coefficient (*Kp*), *n* and *r* Values From In Vitro Release Studies**

Formulation code	Flux (μg/cm^2)	$Kp \times 10^4$	n	$r^{(a)}$
F1P1	1.88	9.22	0.51	0.930
F1P2	1.99	8.26	0.44	0.971
F1P3	1.71	6.10	0.53	0.968
F2P2	2.31	8.11	0.42	0.931
F2P3	2.56	5.39	0.41	0.986
F3P1	2.10	8.94	0.47	0.891
F3P2	1.92	8.53	0.46	0.978

[(a)]r is correlation coefficient calculated at 95% confidence limit.

With the release of surface drug, numerous pores and channels are possibly generated in the matrix structure, which further elevates the rate and extent of ATL release. Again, as a result of the hydrophilic nature of the polymer, when exposed to diffusion media, free volume spaces are generated between the macromolecular chains. After solvation of the polymer chains, the dimensions of polymer chain will increase because of polymer relaxation. In non-Fickian or anomalous transport, both diffusion as well as macromolecular relaxation time scales are identical and both will control the overall rate of penetrant absorption. Case II transport is the limit when relaxation predominates. However, zero-order, time-independent Case II kinetics are characterized by a linear mass uptake with time.

The steady-state flux (*Jss)* was also calculated from the slope of the linear portions of the straight lines obtained by plotting the mean cumulative drug released vs. time. The permeability coefficient (*Kp*) was calculated using the equation (Yammune et al., 1995):

$$Kp = \frac{Jss}{Cs} \tag{6}$$

where *Cs* is the concentration of drug in the transdermal membrane. These results are presented in Table 5. The flux obtained for all the formulations ranged between 1.71 and 2.56 μg/cm^2, whereas *Kp* values varied from 5.39×10^{-4} to 9.22×10^{-4}.

CONCLUSIONS

The present study demonstrates the use of modified xanthan films to develop transdermal patches. Acrylamide was successfully grafted onto XG by the free radical polymerization using ceric ion initiator. FT-IR spectroscopy and DSC indicated the formation of the graft copolymer. The films casted by using the graft copolymer, plasticizer, and ATL by solution casting method were slightly opaque, smooth, flexible and were permeable to water vapor, indicating their favorable permeability characteristics. FT-IR and DSC studies indicated no significant interactions between ATL and the polymer matrix; drug was distributed uniformly throughout the matrix with a slight amorphous morphology. X-RD indicated that the drug inside the film was not completely in the crystalline form. SEM studies of the placebo and drug-loaded films demonstrated a remarkable change in surface morphology. The skin irritation test results suggested that both the placebo and the drug-loaded films have produced negligible erythema and edema compared to formalin (0.8% v/v) as a standard irritant. The in vitro drug release studies showed variations in drug release profiles among the different formulations developed. The obtained *n* values indicated the drug diffusion to follow a Fickian trend. Steady-state flux for in vitro release varied in the range of 1.71–2.56 μg/cm^2, while the *Kp* values varied from 5.39 to 9.22×10^{-4}.

ACKNOWLEDGMENTS

Professor T. M. Aminabhavi wishes to express thanks to the University Grants Commission (UGC), New Delhi, India, for a major funding support (Grant No: F1-41/2001/CPP-II) to establish the Center of Excellence in Polymer Science. We also thank Dr. P. V. Kulkarni and Dr. N. N. Mallikarjuna for providing the SEM photographs.

REFERENCES

Adhikary, P., & Singh, R. P. (2004). Synthesis, characterization, and flocculation characteristics of hydrolyzed and unhydrolyzed polyacrylamide grafted xanthan gum. *J Appl Polym Sci., 94*, 1411–1419.

Banga, A. K., & Chien, Y. W. (1993). Hydrogel-based iontotherapeutic delivery devices for transdermal delivery of peptide/protein drugs. *Pharm. Res., 10*, 697–702.

Behari, K., Pandey, P. K., Kumar, R., & Taunk, K. (2001). Graft copolymerization of acrylamide onto xanthan gum. *Carb. Polym., 46*, 185–189.

Brazel, S. C., & Huang, X. (2001). On the importance and mechanisms of burst release in matrix-controlled drug delivery systems. *J. Control. Rel., 73*, 121–136.

Cho, C-W., & Shin, S-C. (2004). Enhanced transdermal delivery of atenolol from the ethylene–vinyl acetate matrix. *Int. J. Pharm., 287*, 67–71.

Jakupec, M. A., Unfried, P., & Keppler, B. K. (2004). Pharmacological properties of cerium compounds. *Rev. Phy. Biochem. Pharm., 1*, 101–111.

Karadag, E., Saraydin, D., Cetinkaya, & S., Guven, O. (1996). In vitro swelling studies and preliminary biocompatibility evaluation of acrylamide-based hydrogels. *Biomaterials., 17*, 67–70.

Kim, J., & Shin, S-C. (2004). Controlled release of atenolol from the ethylene-vinyl acetate matrix. *Int. J. Pharm., 273*, 23–27.

Makarand, V. R., & Bhonde, R. R. (2000). Polyacrylamide-chitosan hydrogels: In vitro biocompatibility and sustained antibiotic release studies. *Drug Delivery., 7*, 69–75.

Mundargi, R. C., Agnihotri, S. A., Patil, S. A., & Aminabhavi,T. M. (2006). Graft copolymerization of methacrylic acid onto guar gum using potassium persulfate as an initiator. *J Appl Polym Sci., 101*, 618–623.

Peppas, N. A., & Khare, A. R. (1993). Preparation, structure and diffusional behavior of hydrogels in controlled release. *Adv. Drug Del. Rev., 11*, 1–35.

Rao, P. R., & Diwan, P. V. (1997). Permeability studies of cellulose acetate free films for transdermal use: Influence of plasticizers. *Pharm. Acta. Helv., 72*, 47–51.

Ritger, P., & Peppas, N. (1987). A simple equation for description of solute release: II. Fickian and anomalous release from swellable devices. *J. Control. Rel., 5*, 37–42.

Sarpotdar, P. P., & Zatz, J. L. (1986). Percutaneous absorption enhancement by nonionic surfactants. *Drug Dev. Ind. Pharm., 12*, 1625–1647.

Shin, S-C., & Choi, J-S. (2003). Enhanced bioavailability of atenolol by transdermal administration of the ethylene vinyl acetate matrix in rabbits. *Eur. J. Pharma. Biopharm., 56*, 439–443.

Valenta, C., & Auner, B. G. (2004). The use of polymers for dermal and transdermal delivery. *Eur. J. Pharm. Biopharm., 58*, 279–289.

Wilkinson, J. B., & Moore, R. J. (1989). *Harry's Cosmeticology*. Longman Scientific and Technical: England; 38–39.

Williams, A. C., Barry, B. W. (2004). Penetration enhancers. *Adv. Drug Del. Rev., 56*, 603–618.

Yammune, M. A., Williams, A. C., Barry, B. W. (1995). Terpenes penetration enhancers in propylene glycol/water co-solvent systems: Effectiveness mechanism of action. *J. Pharm. and Pharmacol., 47*, 978–989.